Multiplicity distributions in $\bar{\nu}_\mu p$ interactions

M. Derrick, P. Gregory,* F. LoPinto,† B. Musgrave, J. Schlereth, P. Schreiner,† and R. Singer†

Argonne National Laboratory, Argonne, Illinois 60439

S. J. Barish,‡ R. Brock,§ A. Engler, T. Kikuchi, R. W. Kraemer, F. Messing, B. J. Stacey,‖ and M. Tabak

Carnegie-Mellon University, Pittsburgh, Pennsylvania 15213

V. E. Barnes, T. S. Carman, D. D. Carmony, C. Davis, E. Fernandez,** A. F. Garfinkel, and A. T. Laasanen

Purdue University, West Lafayette, Indiana 47907

(Received 21 September 1981)

We present the multiplicity distributions of the hadrons produced in antineutrino-proton interactions. The data sample, which consists of 2025 charged-current events with antineutrino energy greater than 5 GeV, comes from exposures of the 15-foot hydrogen bubble chamber to the broad-band antineutrino beam at Fermilab. The distribution in hadronic mass W has an average value of 3.7 GeV but extends up to 10 GeV. The mean multiplicity of charged hadrons depends on the hadronic mass W and varies as $\langle n_{ch} \rangle = (-0.44 \pm 0.13) + (1.48 \pm 0.06) \ln W^2$ for $W^2 > 4$ GeV^2. The mean multiplicities for events with three or more charged tracks averaged over the total data sample are $\langle n_- \rangle = 1.68 \pm 0.03$ and $\langle n_0 \rangle = 1.11 \pm 0.07$ for π^- and π^0 production, respectively. The mean π^0 multiplicity is found to increase slowly with n_-. The integrated correlation coefficient f_2^{--} and the dispersion D^- are given as a function of n_-. When compared to the distributions characteristic of other leptonic and hadronic reactions, we find a similarity between the $\bar{\nu}$ data and results from hadronic reactions that have no diffractive component. Multiplicity data for the heavier particles K^0, ρ^0, and Λ are also summarized. The pion multiplicities in the current fragmentation region exceed those for the target fragmentation at all W values. They also satisfy the isospin relation $2\langle n_0 \rangle = \langle n_+ \rangle + \langle n_- \rangle$ required for the fragmentation of an $I = \frac{1}{2}$ quark when a $W > 4$ GeV selection is imposed.

I. INTRODUCTION

In this paper, we present our final results on the multiplicity distributions of antineutrino-proton interactions. In a previous paper,[1] we gave our first results based on about 20% of the present data sample. In that analysis, the overall features of the data were found to be similar to those of other multiparticle reactions when compared at the same values of hadronic c.m. energy. However, the width of the multiplicity distribution was more similar to that observed in the $\bar{p}p$ annihilation process than to that characteristic of hadronic reactions having a strong diffractive component. This is consistent with the known small diffractive production of the ρ and A_1 resonances in neutrino reactions at present energies.[2]

The higher statistics of our complete sample allow a more detailed comparison with results from hadronic reactions[3] as well as data from e^+e^- annihilations[4] and νp interactions.[5]

II. EXPERIMENTAL DETAILS

The data sample was obtained from three separate exposures of the Fermilab 15-foot hydrogen bubble chamber. Most of the 226 000 pictures used in the experiment were obtained with a 400-GeV proton beam incident on an aluminum target. Two horns were used to focus the produced negative particles which in turn decayed to generate the $\bar{\nu}_\mu$ beam. The ν_μ background flux was at the 10% level except at the highest neutrino energies.

In the scanning process, we selected all events with three or more prongs for which the total momentum in the forward hemisphere exceeded 2 GeV/c. The overall scanning and event-

reconstruction efficiencies averaged ~90% and ~95%, respectively. Multiplicity-dependent multipliers were applied to correct for these losses.

The $\bar{\nu}p$ charged-current (CC) events were extracted from the sample that includes contributions from both CC and neutral-current (NC) reactions

$$\bar{\nu}p \to \mu^+ H^0 , \qquad (1)$$

$$\nu p \to \mu^- H^{++} , \qquad (2)$$

$$\bar{\nu}p \to \bar{\nu}H^+ , \qquad (3)$$

$$\nu p \to \nu H^+ . \qquad (4)$$

Backgrounds from K_L^0 mesons and neutrons are small and can be ignored by selecting events in which the charged tracks have a total momentum ≥ 5 GeV/c.[6]

Empirical muon selection criteria for the separation of CC and NC events have been developed in a Monte Carlo (MC) simulation of the experiment.[7] The selection depends essentially on the difference in both the total and the transverse momentum of the muon as compared to the hadronic tracks. The measurement of the beam energy for events with missing neutrals was made by parametrizing the events in terms of the transverse momentum of the missing-neutral system relative to the direction of the total hadronic system. The resolution in neutrino energy is about $\pm 10\%$; however, the total hadronic energy W is less well determined.

We also apply the selection $0.1 \leq y < 0.8$ to the complete sample, where $y = (E_{\bar{\nu}} - E_\mu)/E_{\bar{\nu}}$ is the usual scaling variable. Our MC studies show that this selection is needed to minimize the backgrounds and ensure good efficiency in selecting the $\bar{\nu}p$ CC events.[7] It was not applied in our earlier study[1] based on a much smaller event sample. No selection is made on the Bjorken x variable. Hadrons with laboratory momentum less than 1 GeV/c, which are identified as protons through ionization density in the chamber, are called protons; all other charged hadrons are assigned the pion mass.[8]

In order to present distributions where the effects of instrumental smearing from measurement uncertainties, muon selection, and neutrino-energy determination are minimized, we also apply the MC simulation to measure the correction factors. The program is run first with no measurement uncertainties on the tracks and with known muon identity and neutrino energy, and then it is run with these uncertainties included. Comparison of the results from the two runs measures the correc-

tion function for the particular variable. The program incorporates the known distributions in (x, y) at the lepton vertex as well as the multiplicity distributions of charged and neutral secondaries as measured in our first experiment. The nucleons are generated according to the observed Feynman x distribution. With the y selection, the background is calculated to be 11% and the detection efficiency 90%. These numbers are somewhat worse than for the sample used in our analysis of inclusive scattering[7] where we imposed the additional selection that $x > 0.1$.

One-prong events are not included in the data sample. However, at low W it is important to correct for these events and we have included a one-prong sample generated from the MC simulation. Our studies of the constrained channels with a small number of final-state hadrons such as $\mu^+ p \pi^-$ (Ref. 9) and $\mu^+ p \pi^- \pi^+ \pi^-$ show that these events occur predominantly at low values of W. The cross sections are dominated by N^* and Δ production and so are relatively flat with antineutrino energy, $E_{\bar{\nu}}$. As the multiplicity of the final state increases, the y distribution becomes broader as shown by the comparison of single $(p\pi^-)$ and triple $(p\pi^- \pi^+ \pi^-)$ pion production in Fig. 1(a) and 1(b), respectively. In Fig. 1(c) and 1(d), we show
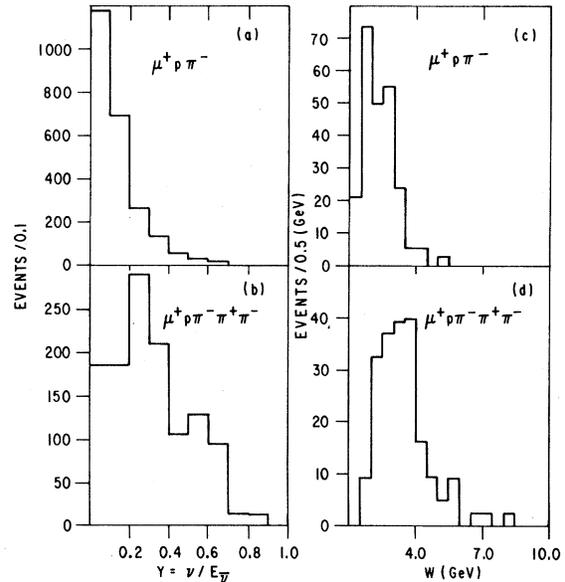

FIG. 1. The distributions in $y = \nu/E_{\bar{\nu}}$ for (a) the $\mu^+ p \pi^-$ final state and (b) the $\mu^+ p \pi^- \pi^+ \pi^-$ final state. The distribution in hadronic mass W selected with $0.1 \leq y < 0.8$ for (c) the $\mu^+ p \pi^-$ final state and (d) the $\mu^+ p \pi^- \pi^+ \pi^-$ final state.

the distributions in W for the same events with the cut $0.1 \leq y < 0.8$. As expected, the $\mu^+ p \pi^-$ events occur at lower W values than do the $\mu^+ p \pi^- \pi^+ \pi^-$ events.

The one-prong events populate the final states $\mu^+ n \pi^0$, $\mu^+ n \pi^0 \pi^0$, etc., and it is reasonable to expect that the W dependence of the states involving neutral pions will be similar to the fitted channels involving a small number of charged pions. The dashed curve in Fig. 2 shows the W variation of the ratio $= (\mu^+ p \pi^- + \mu^+ p \pi^- \pi^+ \pi^-)/\mu^+ X^0$, where X^0 contains at least two charged particles. The solid curve shows the results of the MC prediction for the ratio $= \mu^+ N^0 / \mu^+ X^0$, where N^0 contains only neutral hadrons. The latter numbers are used to make the one-prong event correction as a function of W. Both ratios are calculated with the cut $0.1 \leq y < 0.8$.

The shapes of the two distributions are quite similar, although the fraction of fitted events is less peaked at low W than is the neutral distribution because the former does not contain any simulation of the $\mu^+ n \pi^0 \pi^0$ final state. The uncertainty on the dashed line is large since it is based on a small number of fitted events. Above about 3 GeV, the two ratio distributions agree quite well. Since there is no unique way to estimate the absolute cross sections for the multineutral final states, this similarity of the two distributions for the higher W values could not have been predicted. We assign an arbitrary 10% scale uncertainty to the MC estimation of the zero-prong correction.
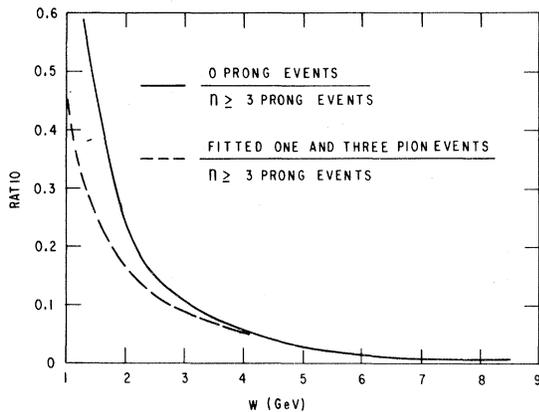

FIG. 2. The W dependence of the ratio of the sum of the $\mu^+ p \pi^-$ and $\mu^+ p \pi^- \pi^+ \pi^-$ events to all CC events with ≥ 3 prongs is shown as the solid curve. The dashed curve shows the MC result for the W dependence of the ratio of CC events with only neutral hadrons to all CC events with ≥ 3 prongs.

Since we are only concerned with values of $W^2 > 4$ GeV^2, the differences at low W are not important.

For each $\bar{\nu}p$ and νp charged-current event, a search was made for associated V^0's pointing to the main vertex. These particles were either neutral-hadron decays (K^0, Λ, $\bar{\Lambda}$) or γ-ray pair conversions. After a detailed analysis of these data,[10] we obtained a sample of 233 (116) γ conversions, 82 (23) K_S^0, and 44 (6) Λ decays associated with the $\bar{\nu}p$ (νp) CC samples.

III. DEFINITION OF VARIABLES

We use the usual set of variables to describe the kinematics at the lepton vertex. These are the four-momentum transfer Q^2, the energy transfer $\nu = E_{\bar{\nu}} - E_{\mu}$, the Bjorken scaling variable $x = Q^2/2M\nu$, where M is the nucleon mass, and the energy-sharing variable $y = \nu/E_{\bar{\nu}}$ where $E_{\bar{\nu}}$ and E_{μ} are the incident-neutrino and secondary-muon energies, respectively. At the hadron vertex, W is the effective mass of all final-state hadrons. This quantity also measures the c.m. energy in the current-nucleon rest system.

The variables are related by the equation

$$W^2 = M^2 + Q^2 \left[\frac{1}{x} - 1 \right] .$$ (5)

In the hadronic c.m. system, the Feynman variable X_F is given by

$$X_F = \frac{2P_L^*}{W} ,$$ (6)

where P_L^* is the longitudinal momentum in this system.

The relationships among x, y, and W for typical values of the antineutrino energy are shown in Fig. 3. The solid curves show the constant W contours while the dashed lines indicate the cuts made in y. The data are only used in the y range $0.1 \leq y < 0.8$. As we have discussed, the data with $y < 0.1$ contain many of the one-prong events with an all neutral hadronic system. For high y, $y > 0.8$, the efficiency for detection of the muon decreases, and so the contamination in the sample of charged-current events from the neutral-current sample is large. As can be seen from Fig. 3, these cuts on y modify the W distribution. However, since the multiplicity depends primarily on W and since the data will be discussed in W bins, this y selection does not *a priori* affect the results.
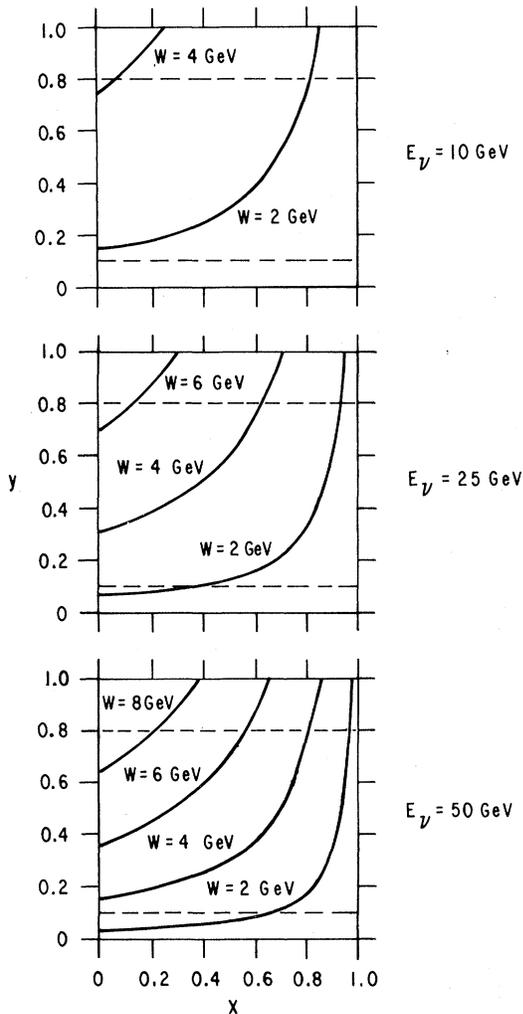
FIG. 3. Contours of fixed W on the x,y plots for different neutrino-energy selections.

IV. RESULTS

The basic data from the experiment are given in Table I, where we tabulate the number of events, corrected for scanning and measuring losses, with their statistical errors as a function of W and prong number. The total numbers of raw and corrected events with $\langle n_{ch} \rangle \geq 2$ in the sample after these selections are 2025 and 2568, respectively. The one-prong events with $n_{ch} = 0$, listed in Table I, are the MC estimates.

The bulk of the charged-current data are in the W range, $2 < W < 6$ GeV with a median W value of 3.7 GeV. The Q^2 distribution falls monotonically and has a mean value of 4.5 $(\text{GeV}/c)^2$.[8] The mean overall negative-particle multiplicities are

$\langle n_- \rangle = 1.68 \pm 0.03$ for events with $n_{ch} \geq 2$ and $\langle n_- \rangle = 1.52 \pm 0.03$ when the one-prong correction is included.

The multiplicity can, in principle, be dependent on a number of variables, and the Q^2 dependence of $\langle n_{ch} \rangle$ is shown in Fig. 4, for both the total event sample and for the events with $W > 3$ GeV. The charge multiplicity for the total sample increases slowly with Q^2. Since W^2 and Q^2 are related by Eq. (5), and since the mean x value of the data is ~ 0.25, Q^2, and W^2 are strongly correlated at low W^2 values. If the data are restricted to $W > 3$ GeV, the dependence of $\langle n_{ch} \rangle$ on Q^2 is removed, as seen in Fig. 4(a).

There is, however, a strong dependence of $\langle n_{ch} \rangle$ on W as seen in Table I and Fig. 5. The data points are plotted at the mean W^2 value of the events in each bin, and the points shown have been corrected for background, instrumental smearing, and muon-detection efficiency. They also include the one-prong correction. A fit over the range $4 < W^2 < 100$ GeV^2 gives

$$\langle n_{ch} \rangle = (-0.44 \pm 0.13)$$
$$+ (1.48 \pm 0.06)\ln W^2 ,$$

as shown by the solid curve in Fig. 5. This W^2 range excludes the lowest W region where the largest one-prong correction is made. The dashed curve shows the fit to the results of Allen et al. from a νp experiment.[5] In this case also, the linear dependence on $\ln W^2$ sets in above $W^2 = 4$ GeV^2 and the slope of 1.33 ± 0.02 is smaller than we measure.[11] Since the hadronic system has a net charge of $+2$ (0) in the νp ($\bar{\nu}p$) case, one expects a difference at low W. Neutrino-proton reactions at low energy are characterized by strong Δ^{++} production, so the three-prong topology is enhanced. For the higher W values, the νp and $\bar{\nu}p$ charged multiplicities become equal.

The long-dashed—short-dashed curve shows the trend of the e^+e^- annihilation data.[4,12] Although these data are in reasonable agreement with the neutrino results for the higher W values of our experiment, at low W, the e^+e^- multiplicities exceed the neutrino values. The e^+e^- multiplicity data from the ADONE storage ring[12] are not corrected for the unseen, all neutral annihilations, nor do they include the contributions from the $\pi^+\pi^-$ or K^+K^- final states. In the neutrino case, of course, baryon conservation significantly reduces the energy available for meson production. Although the e^+e^- data can be fit with an $a + b \ln W$ form in the W range shown in Fig. 5 at

TABLE I. Event distributions in prong numbers and W.

W range (GeV)	$n_{ch}=0$[a]	2	4	6	8	10	$\langle n_{ch} \rangle$	f_2^{--}	D_-
			Correct number of events						
1.0— 1.5	15.8	28.7± 6.1	0	0	0	0	1.29±0.15	−0.42±0.14	0.48±0.13
1.5— 2.0	80.4	209.4±16.6	13.9± 4.0	0	0	0	1.61±0.06	−0.49±0.08	0.56±0.07
2.0— 2.5	69.9	316.7±20.3	68.6± 8.9	2.8± 2.0	0	0	2.10±0.06	−0.65±0.10	0.63±0.08
2.5— 3.0	53.3	272.1±18.8	131.0±12.3	6.7± 3.0	0	0	2.49±0.07	−0.75±0.13	0.71±0.09
3.0— 3.5	36.9	226.5±17.2	157.7±13.5	23.7± 5.8	1.8±1.8	0	2.88±0.08	−0.82±0.18	0.79±0.12
3.5— 4.0	20.7	98.8±11.3	154.5±13.4	40.8± 7.4	1.5±1.5	0	3.48±0.10	−1.04±0.26	0.83±0.16
4.0— 4.5	13.0	71.5± 9.7	122.9±11.9	52.8± 8.7	12.7±4.5	0	3.92±0.13	−1.06±0.39	0.95±0.20
4.5— 5.0	6.5	38.3± 7.1	79.9± 9.6	37.6± 7.2	7.0±3.5	0	4.04±0.16	−1.21±0.48	0.90±0.26
5.0— 7.5	9.5	34.8± 6.7	132.7±12.4	93.4±11.3	43.9±8.3	11.0±4.2	5.01±0.14	−1.31±0.52	1.10±0.24
7.5—10.0	0.3	5.2± 2.6	14.1± 4.1	23.1± 5.8	13.6±4.6	4.0±2.8	5.90±0.33	−1.73±1.44	1.10±0.65
Totals	306.1	1302	875.3	280.9	80.5	15			

[a]Estimated from the Monte Carlo simulation.

higher energies, the e^+e^- data lie well above an extrapolation of such a fit.[4] This may be connected to the increasing importance of gluon fragmentation as the energy is increased. If this is the case, then higher-energy neutrino data should show a similar, although less dramatic, growth.

Multiplicities measured in hadronic collisions are also about the same as those shown in Fig. 5. Specifically, the measured pp and $\bar{p}p$ multiplicities[3] bracket the lepton data in this W range. A similar comparison of our $\bar{\nu}p$ results and the hadronic data is seen in Fig. 6, where we display the variation of

the mean negative-particle multiplicity $\langle n_- \rangle$ with W^2. The lines show the trends of the pp data and the annihilation data.[1] Our $\bar{\nu}p$ data behave similarly to the annihilation data, although the absolute values of $\langle n_{ch} \rangle$ are somewhat lower. This may again be connected to the presence of a baryon in the $\bar{\nu}p$ final states. The pp results, by contrast, show rapidly rising values of $\langle n_- \rangle$ with W^2 at small W^2, but the data lie much below the other results. In the pp case about 2 GeV of c.m. energy remains in the baryon masses, but the differences at the higher W values are a reflection of the large diffractive component in pp interactions that pre-
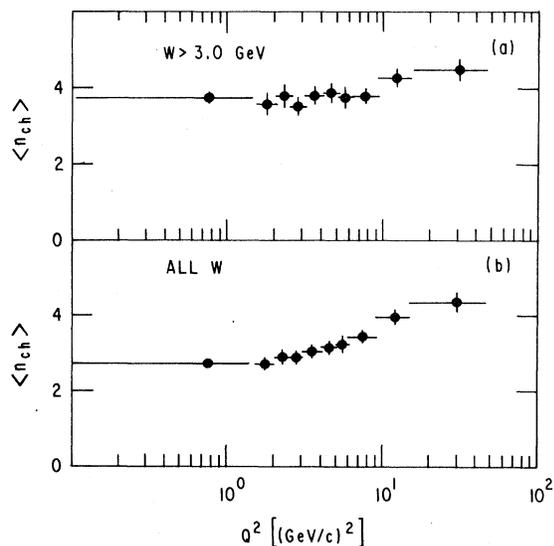

FIG. 4. The mean charged-hadron multiplicity $\langle n_{ch} \rangle$ as a function of Q^2 for (a) $W \geq 3$ GeV and (b) all W.
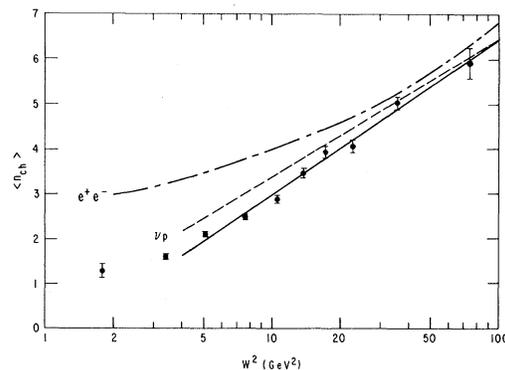

FIG. 5. The mean charged-hadron multiplicity $\langle n_{ch} \rangle$, as a function of hadronic mass squared W^2. The $\bar{\nu}p$ data of this experiment is shown by the data points and compared to parametrizations of the νp data (dashed curve) and e^+e^- annihilation data (long-dashed—short-dashed curve). The solid curve is the fit to our $\bar{\nu}p$ data for $W^2 > 4$ GeV².
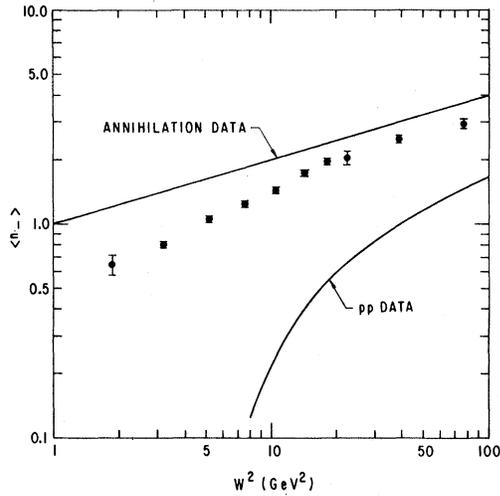
FIG. 6. The W^2 variation of mean negative-hadron multiplicity $\langle n_- \rangle$. The $\bar{\nu}p$ results of this experiment, shown by the data points, are compared to pp and $\bar{p}p$ annihilation results.

ferentially feeds the low multiplicities.

These differences are also exhibited in the variation with $\langle n_- \rangle$ of the integrated correlation function f_2^{--} defined as

$$f_2^{--} = \langle n_-(n_- - 1) \rangle - \langle n_- \rangle^2 . \tag{7}$$

This parameter measures the width of the multiplicity distribution and is zero for a pure Poisson shape. As shown in Fig. 7, f_2^{--} for our data fall as $\langle n_- \rangle$ increases, implying that the multiplicity
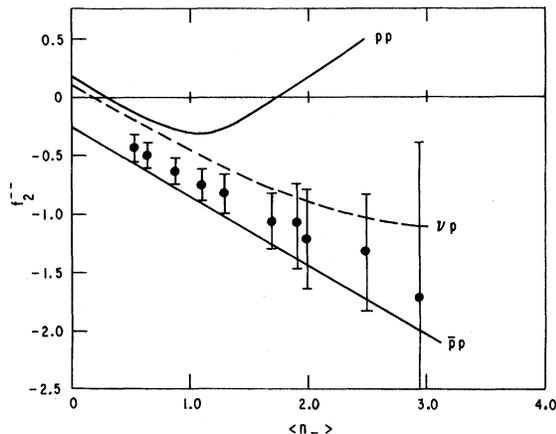

FIG. 7. The variation of the correlation coefficient f_2^{--} with $\langle n_- \rangle$. The $\bar{\nu}p$ results of this experiment, shown by the data points, are compared to νp results (dashed curve) as well as to pp and $\bar{p}p$ annihilation results.
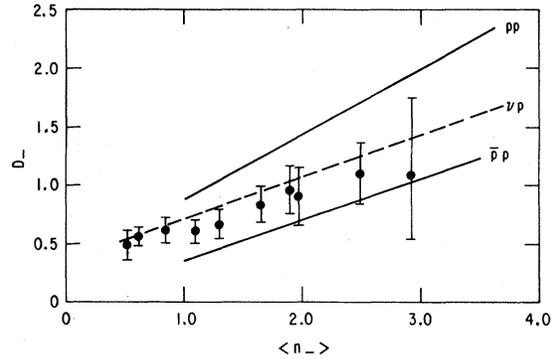

FIG. 8. The variation of the dispersion D_- with $\langle n_- \rangle$. The $\bar{\nu}p$ data of this experiment, shown by the data points, are compared to νp results (dashed curve) as well as to pp and $\bar{p}p$ annihilation results.

distribution narrows as $\langle n_- \rangle$ increases. Similar behavior is seen in both the νp data and in the $\bar{p}p$ data.[13] In contrast, the strong diffractive component in pp interactions causes the multiplicity distribution to broaden as the energy increases and f_2^{--} becomes positive as $\langle n_- \rangle$ increases.

Similar comparisons are seen in Fig. 8 where we plot the dispersion D_- defined as

$$D_- = (\langle n_-^2 \rangle - \langle n_- \rangle^2)^{1/2} . \tag{8}$$

Both our $\bar{\nu}p$ data and the results from νp, pp, and $\bar{p}p$ interactions are consistent with a linear fit $D_- = a + b\langle n_- \rangle$. The slope b varies from 0.36 for the νp and $\bar{p}p$ data to 0.58 for the pp case. Our $\bar{\nu}p$ data give a slope of 0.31 ± 0.12, in agreement with the νp and $\bar{p}p$ values.

The mean π^0 multiplicity has been measured for both the $\bar{\nu}p$ and the νp CC events in our experiment by using the observed number of γ-ray conversions. The necessary corrections to convert the γ-ray count to the π^0 multiplicity were determined by taking the negative tracks at the primary vertex, and (assuming that they are π^0) allowing them to decay to $\gamma\gamma$. Since low-energy $e^+ e^-$ pairs are difficult to handle, a minimum-laboratory-momentum cut of 200 MeV/c was imposed on the γ-ray momentum spectrum. This correction is multiplicity-dependent, falling from 22% for 3-prong events to 13% for 11-prong events. Figure 9 shows the observed γ-ray spectrum, together with the prediction using the negative-track simulation. The loss of low-momentum γ rays is evident. In addition to this cut, we required a minimum γ-ray flight path of 1 cm in order to have a clear conversion vertex. With these selections, the mean γ
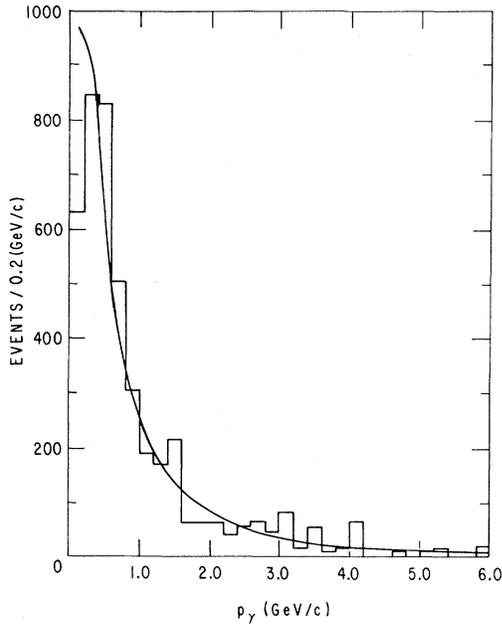
FIG. 9. The momentum distribution of the converted photons, shown in the histogram, compared to the spectrum calculated using the negative tracks shown by the curve.

weights were 16.3 and 14.7 for $\bar{v}p$ and vp interactions, respectively.

The resulting sample of observed γ conversions, classified according to the multiplicity at the primary vertex and to a $\bar{v}p$ or vp CC interaction is given in Table II. Under the assumption that all γ rays arises from π^0 decay, the mean overall π^0 multiplicities $\langle n_0 \rangle$ are 1.11 ± 0.07 and 1.66 ± 0.05 for $\bar{v}p$ and vp CC interactions, respectively. The clear increase of mean π^0 multiplicity $\langle n_0 \rangle$ with

prong number n_-, is shown in Fig. 10 and can be parametrized as

$$\bar{v}p: \quad \langle n_0 \rangle = (0.72 \pm 0.18)$$
$$+ (0.22 \pm 0.10)n_- ,$$

$$vp: \quad \langle n_0 \rangle = (0.14 \pm 0.30)$$
$$+ (0.73 \pm 0.16)n_- .$$

These results are in agreement with our findings based on the first sample of film[1] and with the published vp results of Chapman *et al.*[5] They are in some disagreement with $\bar{v}$ neon data of Ammosov *et al.*[14] who found $\langle n_0 \rangle$ to be independent of n_-, although the mean π^0 multiplicity of $\langle n_0 \rangle = 1.2 \pm 0.05$ measured in that experiment is in agreement with our result.

A compilation of π^0 multiplicities measured in hadronic experiments[15] shows a correlation of $\langle n_0 \rangle$ with n_-, which is flat or slightly negative for low c.m. energies, but which becomes positive as the beam energy increases, with a slope parameter reaching 0.7 for W values in the $20-40$ GeV range. Considering that our experiment is done over a range of c.m. energies, our positive slope parameter is in agreement with these observations.

We have also measured the neutral-strange-particle production rates.[10] The corrections, which include the scanning and reconstruction losses as well as the minimum-length cut at 1 cm, lead to a mean weight of 1.6 for a neutral-hadron event. The rate for events to contain at least one V^0 are

$$\frac{\bar{v}p \rightarrow \mu^+ V^0 X^0}{\bar{v}p \rightarrow \mu^+ X^0} = 0.16 \pm 0.03 ,$$

TABLE II. Neutral-pion multiplicities.

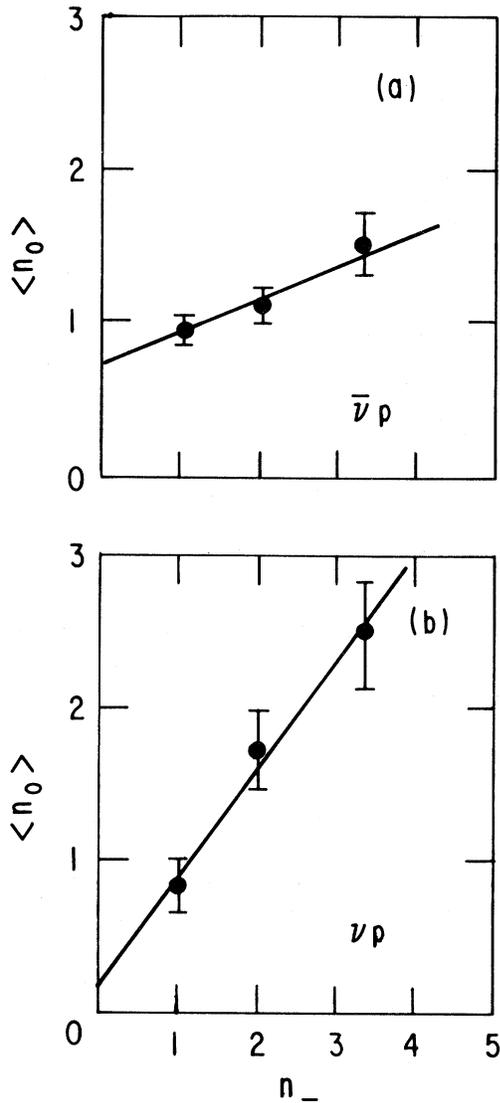| Charged-hadron multiplicity	Number of events with converted γ ray	Corrected number of events	$\langle n_0 \rangle$
Antineutrino-proton			
2	1073	2055.1 ±206	0.96±0.10
4	798	1790.8 ±187.7	1.12±0.12
≥6	261	787.4 ±121.4	1.51±0.23
Neutrino-proton			
2	189	312.4± 68.2	0.83±0.18
4	257	887.2±126.7	1.73±0.25
≥6	173	856.1±126.2	2.47±0.36

FIG. 10. Mean π^0 multiplicity $\langle n_0 \rangle$ as a function of n_- for (a) $\bar{\nu}p$ interactions and (b) νp interactions.
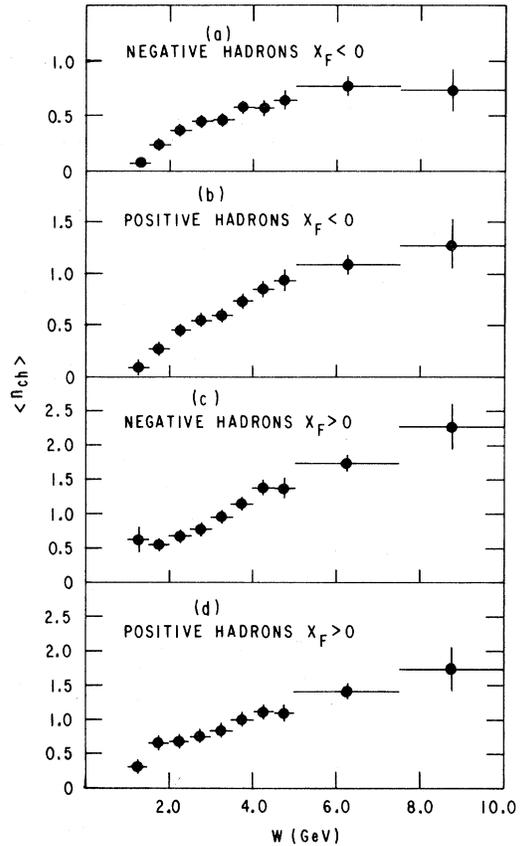

FIG. 11. Mean hadron multiplicity as a function of W for (a) negative hadrons with $X_F < 0$, (b) positive hadrons with $X_F < 0$, (c) negative hadrons with $X_F \geq 0$, and (d) positive hadrons with $X_F \geq 0$.

and

$$\frac{\nu p \to \mu^+ V^0 X^{++}}{\nu p \to \mu^- X^{++}} = 0.15 \pm 0.04 \ .$$

These numbers, which are in good agreement with other measurements of strange-particle production in neutrino experiments,[16] can be broken down into K^0 (0.12$\pm$0.03) and Λ^0 (0.04$\pm$0.01) for the $\bar{\nu}p$ case. The K^0 rate may be compared to the multiplicity of ρ^0 production of 0.21$\pm$0.03 in our $\bar{\nu}p$ CC events.[17]

Since the hadronic system in $\bar{\nu}p$ scattering is neutral, one would expect about 0.5 protons per

event, at least in the higher multiplicities, consistent with our earlier estimate of 0.53$\pm$0.15 based on a comparison of the $\bar{\nu}p$ and νp fragmentation functions and assuming charge independence.[1]

Since $\bar{\nu}p$ CC reactions are thought to proceed via a $u \to d$ quark transition followed by d-quark fragmentation, it is, in principle, possible to measure the properties of d-quark fragmentation in an experiment such as ours.[18] There are, however, experimental difficulties that stem from the lack of a clean separation between the current and the target fragmentation regions at available energies.[8] Ignoring these problems and merely making a selection of hadrons, forwards or backwards in the c.m. system as belonging to the quark or diquark systems, results in the distributions of Fig. 11, where $\langle n_\pm \rangle$ is shown as a function of W. The forward multiplicities of $\langle n_+ \rangle = 0.87 \pm 0.02$ and $\langle n_- \rangle = 1.02 \pm 0.02$ exceed the backward values of $\langle n_+ \rangle = 0.65 \pm 0.02$ and $\langle n_- \rangle = 0.50 \pm 0.02$, and

this is true of all W values. This difference of the forward and backward multiplicities is also seen in the vp data of Allen *et al.*,[5] as well as in a recent vd experiment.[19] The result suggests a different mechanism for d-quark fragmentation as compared to the breakup of the ud diquark system which may be contrasted to the similarity of the kinematic distributions as measured by thrust and sphericity.[20]

Since we do not detect a truly inclusive sample of π^0s, i.e., photons from all neutral hadronic final states are not included, it is not possible to make a general test of the relationship $2\langle n_0 \rangle = \langle n_+ \rangle + \langle n_- \rangle$ which is required for the fragmentation of an $I = \frac{1}{2}$ system into pions. We can, however, make the test in a limited kinematic range. Figure 2 shows that the one-prong correction is small for events with $W \geq 4$ GeV. In our previous studies,[8] we found that this W cut is also required to separate the current fragments from the target fragments. The mean W value for this data sample is 5.35 GeV. We separate the converted γ rays into those forwards and those backwards in the hadronic c.m. system and count the γ rays as originating from π^0s in those hemispheres. This selection gives forward and backward π^0 multiplicities for $\langle W \rangle = 5.35$ GeV of $\langle n_0 \rangle = 1.41 \pm 0.15$ and 0.91 ± 0.10, respectively. A calculation, in which we assume that the π^0 rapidity distribution is simulated by that of the π^- shows that the correction needed for decay γ rays that end up in the opposite hemisphere from the original π^0 is negligible. The equivalent mean forward charged multiplicities are $\langle n_+ \rangle = 1.28 \pm 0.06$ and $\langle n_- \rangle = 1.57 \pm 0.07$.

Before comparing to the isospin relation, some corrections must be made, the most important of which is for protons. Our study of particle production[8] shows that although the baryons preferentially populate the backward c.m. hemisphere, a significant fraction are produced with $x_F > 0$. The

European Muon collaboration has recently reported[21] forward proton production in high-energy μp collision with a p/π ratio of ~ 0.1. We therefore reduce the forward positive multiplicity by $(10 \pm 5)\%$ and get charged pion multiplicities for $x_F > 0$ and $W > 4$ GeV of $\langle \pi_+ \rangle = 1.15 \pm 0.09$, $\langle \pi_- \rangle = 1.57 \pm 0.07$. After making the small correction for the π^0s produced in the one-prong events, we measure $\langle \pi_0 \rangle = 1.38 \pm 0.15$. These pion multiplicities clearly satisfy the isospin relation. We have no simple way to correct for the strange-particle contamination but estimates based on the measured production rates[10] of K^0 and Λ^0 show that this correction will be small compared to our statistical errors.

IV. CONCLUSIONS

The results of this experiment confirm our previous findings that antineutrino-nucleon collisions lead to multiplicity distributions that are similar, although not identical, to those observed in $N\bar{N}$ annihilation. The average multiplicities are also quite similar to those observed in other multiparticle reactions. There is a clear difference in the mean multiplicity of the forward-going quark system as compared to the backward-going diquark system. The forward neutral-pion multiplicity is equal to the average of the π^+ and π^- multiplicities.

V. ACKNOWLEDGMENTS

*Present Address: CERN, EP Division, Geneva 23, Switzerland.

†Present Address: Bell Telephone Laboratories, Naperville, Illinois 60540.

‡Present Address: U. S. Department of Energy, Washington, D. C. 20545.

§Present Address: Fermi National Accelerator Laboratory, Batavia, Illinois 60510.

¶Present Address: University of Toronto, Department of Physics, Ontario, M5S 1A7, Canada.

¶Present Address: Lawrence Livermore Laboratory, University of California, Livermore, California 94550.

**Present Address: Argonne National Laboratory, Argonne, Illinois 60439.

[1]M. Derrick *et al.*, Phys. Rev. D **17**, 1 (1978).

[2]J. Bell *et al.*, Phys. Rev. Lett. **40**, 1226 (1978).

[3]E. Albini *et al.*, Nuovo Cimento **32A**, 101 (1976).

[4]Ch. Berger *et al.*, Phys. Lett. **95B**, 313 (1980).

[5]J. W. Chapman *et al.*, Phys. Rev. Lett. 36, 124 (1976); J. Bell *et al.*, Phys. Rev. D 19, 1 (1979); P. Allen *et al.*, Nucl. Phys. B181, 385 (1981).

[6]M. Derrick *et al.*, Phys. Rev. D 18, 17 (1978).

[7]A detailed discussion of the experimental corrections is given in V. E. Barnes *et al.*, Phys. Rev. D 25, 1 (1982).

[8]M. Derrick *et al.*, Phys. Rev. D 24, 1071 (1981).

[9]S. J. Barish *et al.*, Phys. Lett. 91B, 161 (1980).

[10]R. Brock *et al.*, (to be published). R. Brock, Ph.D. thesis, Carnegie-Mellon University, 1980 (unpublished).

[11]In our earlier paper (Ref. 1), a linear fit over the range $1 < W^2 < 50$ GeV^2 gave a slope of 1.22 ± 0.03. The increased precision of the present data shows that the linear fit cannot be extended to such low W values.

[12]C. Bacci *et al.*, Phys. Lett. 86B, 234 (1979).

[13]There is experimental evidence that f_2^{--} for $\bar{p}p$ annihilation turns upwards for higher values of $\langle n_- \rangle$

than are shown in Fig. 7. This upturn is required for a linear variation of D_- with $\langle n_- \rangle$; R. M. Robertson *et al.*, Phys. Rev. D 21, 3064 (1980).

[14]V. Ammosov *et al.*, Nuovo Cimento 51A, 539 (1979).

[15]F. T. Dao and J. Whitmore, Phys. Lett. 46B, 252 (1973).

[16]P. Schreiner, in *Proceedings of the 1979 International Symposium on Lepton and Photon Interactions at High Energies, Fermilab*, edited by T. B. W. Kirk and H. D. I. Abarbanel, (Fermilab, Batavia, Illinois, 1980), p. 291.

[17]M. Derrick *et al.*, Phys. Lett. 91B, 307 (1980).

[18]A similar attempt to measure the multiplicity properties of d-quark jets has been made by V. V. Ammosov *et al.*, Fermilab Report No. Pub-80-96 (unpublished).

[19]T. Kitagaki *et al.*, Phys. Lett. 97B, 325 (1980).

[20]M. Derrick *et al.*, Phys. Lett. 88B, 177 (1979).

[21]J. J. Aubert *et al.*, Phys. Lett. 103B, 388 (1981).